

BIOCOMPATIBILITY AND OSTEOINDUCTIVITY OF THREE DIFFERENT BIOACTIVE MATERIALS: EXPERIMENTAL STUDY

Hayam Y. Hassan^{*}, Manar AA. Selim^{**} and Ahmed M. Negm^{***}

ABSTRACT

Objectives: to investigate the biocompatibility and osteoinductivity of bioactive glass (BAG), mineral trioxide aggregate (MTA) and TheraCal™ LC on bone healing in surgically created defects in rat femurs through histological investigation and immunohistochemical detection of TNF- α as a pro-inflammatory mediator.

Methods: 45 mature rats were divided into 3 experimental groups included three bioactive materials (n=10), a negative control group (n=5) and a positive control group (n=10). The animals were then sacrificed 2 and 5 weeks postoperatively. Histologic evaluations comprising inflammation severity and new bone formation were made on H&E-stained decalcified sections.

Results: Histological results of the experimental groups revealed early processes of bone healing in 2 weeks period but they showed a highly osteoinductive effect at the end of 5 weeks period. The effects of MTA & TheraCal on bone formation both at 2- and 5-weeks period were higher than BAG. **Immunohistochemical** detection of TNF- α of **2 weeks** specimens exhibited strong positive staining reaction of bone marrow tissue for the positive control and three experimental groups with no significant difference. In contrast, Negative to weak immunostaining reactivity of **5 weeks** specimens was observed in the positive control and three experimental groups with no significant difference.

Conclusion: BAG, MTA and TheraCal™ LC bioactive materials are comparable to each other in their biocompatibility and showing bone formation with regression of the inflammatory activity and less fibrous tissue in the repaired region were seen 2 weeks and increased 5 weeks after their implantation. The biocompatibility besides osteoinductivity of BAG and TheraCal™ LC supported their activity as pulp capping, perforation repair and root end filling materials as MTA

Clinical Significance: This experimental study examined biocompatibility besides osteoinductivity of BAG, MTA & TheraCal™ LC through histological investigation and immunohistochemical detection of TNF- α in the function of pro-inflammatory mediator using a rat model.

KEYWORDS: Biocompatibility, Osteoinductive, Bioactive glass, Mineral trioxide aggregate, TheraCal™ LC.

* Associate Professor of Endodontic, Faculty of Dentistry, Suez Canal University, Ismailia, Egypt.

** Associate Professor of Oral Biology, Faculty of Dentistry, Suez Canal University, Ismailia, Egypt.

*** Associate Professor of Endodontic, Faculty of Dentistry, Ahran Canadian University, Giza, Egypt.

INTRODUCTION

Biomaterials have the capability to induce healing and restore the lost tissues within the biological environment ⁽¹⁾. In dentistry, bone defects and injuries that provoke inflammatory response, within 24 hours subsequent the injury and least for one week. Through this complex course, the growth factors and inflammatory signals are emitted in a regulated manner ⁽²⁾. Amounts of some inflammatory mediators, involving interleukin IL-1, IL-6, IL-11, IL-18 and tumor necrosis factor- α (TNF- α), are significantly prominent in the first few days. These signals convert inflammatory cells and advocate angiogenesis. Platelet-derived growth factor and transforming growth factor- β 1 (TGF- β 1) are released through platelets stimulation from the injured blood vessels. Also, bone morphogenetic proteins expressed by Osteoprogenitor cells at the site of fracture ⁽³⁾. All of these factors, beside the inflammatory mediators, employ mesenchyme stem cells and then directed their proliferation and differentiation ^(4,5).

Bioactive glass (BAG) mainly composed of silicate glass (SiO_2), that forming a network oxide where the basic unit is the SiO_4 tetrahedron. This composition supported the Osteoinduction activates on pluripotent stem cells leading to their differentiation to an osteoblastic phenotype ⁽⁶⁾. The upgrade of bioactive glasses explained by Hench et al. in 1969 up till now ⁽⁷⁾. BAG has been integrated into many dental materials as root composite resins, canal sealer and reformative bioactive endodontic materials. Histologically BAG can enhance pulp tissue healing and promote mineralization. Many evidences displayed the capacity of BAG to act as inductive materials for hard tissue development ⁽⁸⁾.

Mineral trioxide aggregate (MTA) is a bioactive material used in treatment of many endodontic cases. MTA made mainly from calcium phosphate, calcium oxide and silicate and bismuth oxide was advanced in 1993 as a retrograde filling material for root-end cavity ⁽⁹⁾. MTA has appropriate biocompatibility

in near contact to pulpal and periapical tissues. It is mainly the material of choice used for pulp capping, root-end filling and perforation repair. Although, MTA has some problems, involving long setting time, difficult handling properties, high price, discoloration potential and questionable antibacterial properties ⁽¹⁰⁾.

TheraCal™ LC (TC) defined as calcium silicate-based material introduced in a single paste light activated marketing as pulp capping liner or base with restorative materials. TheraCal™ LC is based on Portland type III cement (45%), thickening agent as fumed silica (7%), resin (43%), bismuth oxide (3%), and radiopaquer as barium sulfate (3%) ⁽¹¹⁾. TheraCal™ LC has bioavailability through release of calcium ions that responsible for induction, differentiation and proliferation of human dental pulp stem cells and enhance organization and mineralization of hard tissues like structure ^(12,13).

The objective of the current experimental study was to evaluate the biocompatibility, stability and osteoinductivity of three different bioactive materials bioactive glass (BAG), mineral trioxide aggregate (MTA) & TheraCal™ LC (TC) on bone healing in surgically created defects in rat femurs through histological investigation and immunohistochemical detection of TNF- α as a pro-inflammatory mediator using a rat model.

MATERIALS AND METHODS

Synthesis of the bioactive glass powders

Bioactive glass ceramic was carried via a three-step sol-gel method ⁽¹⁴⁾ as follow:

In an well-washed beaker supplied with a magnetic stirrer, 7.63 g calcium nitrate tetra hydrate [$\text{Ca}(\text{NO}_3)_2 \cdot 4\text{H}_2\text{O}$] in 250 ml dry and clean conical flask was dissolved in 120 mL of deionized water at room temperature using magnetic stirrer. The TEOS-ethanol solution was created by diluting, 9.16g of tetraethyl ortho silicates (TEOS) in 60 mL

ethanol and added to calcium nitrate solution and then the nitric acid added adjust the pH value of 1-2 using pH-meter to hydrolyzed TOES solution.

The homogenous solution was slowly dropped into 1500 mL of ammoniated deionized water under vigorous stirring, in which 1.078 g of ammonium dibasic phosphate was dissolved. The pH value of the solution was retained around 10 using ammonia water.

The precipitate was separated from the reaction solution by filtration after stirring 48 h and ageing for 24 h, then, washed three times with deionized water.

The precipitation was freeze dried and got calcination at 700°C in a muffle furnace for 3h, then, the white BAG particles ($\text{SiO}_2\text{-CaO-P}_2\text{O}_5$ (mol %) =55:40:5) were obtained.

Phase analysis by X-ray diffraction (XRD) of bioactive glass particles

Phase's identification of synthesized bioactive glass has been identified using Bruker D8 ADVANCE an X-ray diffractometer (Bruker XRD, Germany) with a $\text{Cu K}\alpha$ ($\lambda = 1.504$ nm) radiation, 40 kV, 25 mA, and 2θ 5-55°.

Particle size distribution report by volume

Particle size distribution reported by volume were measured with a laser dynamic light scattering (DLS) device (Zetasizer Nano ZS, Malvern, UK). Particle size of 1.5mg freshly prepared bioactive glass was verified in ultra-pure deionized water at 25°C. The results were an average of three measurements.

Selection of animals

The present experimental study was conformed to the ARRIVE guidelines. The study protocol was approved by the Ethics Committee of Animal House of the Faculty of Dentistry, Suez Canal University (No.261/2020). Forty-five adult healthy male albino

rats, weighting 150-200 g, were selected and kept corresponding to the guidelines of laboratory animal treatment and care. All the rats were housed in a colony room, each cage contained 5 animals, under a 12 h light/dark cycle, at 25° C, with a free access to tap water and rodent chow.

Anesthesia and surgical procedures:

Five rats of the experimental animals served as negative control (normal) rats while the other forty rats were exposed to the following surgical procedures. General anesthetic procedure for each animal obtained by intraperitoneal injection of 10% Ketamine HCl (Alfasan, Woerden, and the Netherlands) the dose 25 mg/kg body weight and Xylazine (Bayer, Munich, Germany) the dose 0.001 mL/kg body weight.

Allocation of chosen rats

The skin was shaved and disinfected by 70% ethanol at the femur area. Incision was made to get way to rat femur. 1.5 cm incisions were made on the right sides of each rat under aseptic conditions. The noncritical size bone defects were prepared by round carbide bur (D&Z, Wiesbaden, Germany) with low-speed hand piece using normal sterile saline irrigation for each femoral bone in depth of 1 mm and 1.5mm in diameter for implanted materials. After control of bleeding, the positive control group (n=10) the cavities were prepared as mentioned before with no materials placed in them.

The remaining thirty rats were allocated into three main groups (n=10) corresponding to the materials used.

BAG group: The noncritical size bone defects were sealed with bioactive glass (BAG), the powder of the material was carried to the corresponding bony cavity using amalgam carrier.

MTA group: The noncritical size bone defects were filled with MTA (Angelus, Londrina, Paraná, Brazil) incrementally using a Blue MAP system

carrier and were compacted using Buchanan condenser size #1.

TC group: The noncritical size bone defects were filled with TheraCal™ LC (Bisco Inc, Schamburg, IL, USA) which applied into each bony cavity and subjected to light cure for 20 seconds following the manufacturer instructions.

Incision closure

Incisions were sutured by 4-0 silk and the rats were survived under same the environmental conditions. Benzyl penicillin (16000 IU) was given through the intramuscular route, and acetaminophen (1 mg/ml) was administrated by drinking water at the first 2 days after surgery. Stitches were untied at seventh day of surgical process.

After periods of 2 and 5 weeks, 5 animals from positive control group and each experimental group were sacrificed by cervical dislocation after anesthesia and the femoral bones were removed.

Histology and immunohistochemistry:

Femurs of all rats were isolated and kept in 10% buffered formalin. All the femurs were fixed in paraffin blocks after complete decalcification in 10% ethylene diamine tetra acetic acid (EDTA) at room temperature (PH 7-7.4). Afterward, the blocks were dried two times in 70% ethanol. Then at least four times in iso-propylalcohol for one hour each. Successively, the samples were filtrate with liquid paraffin at 56–58 °C, 3 times for one hour. The microtome was used to cut sections 3–5 μm thickness, then fixed on glass slides, stained with hematoxylin and eosin (H&E) and examined under light microscopic.

To examine the inflammatory response after-surgery, **Immunohistochemical** staining for TNF-α was achieved, supplementary sections were examined by indirect IHC. In brief, the sections with no stain were deparaffinized and developed with anti-TNF-α, primary antibody and later

using suitable biotinylated secondary antibody (K1501, Dako, Carpinteria, CA). Positive results of immunoreactivity were identified by ABC complex (PK-6100, Vectastain Elite ABC Kit, Vector Laboratories Inc., Burlingame, CA) after incubation with AEC chromagen (K346911-2, Dako, Carpinteria, CA). The microphotographs were taken using Olympus BX51 (400 X magnification lens, UPLanFL, Olympus). The comparative intensity of TNF-α staining was investigated by viable software Image-Pro plus 6 and counted by (the mean optical density of staining signal × per percent area positively stained × 100)⁽¹⁵⁾.

Statistical Analysis

One-way ANOVA was analyzed and compared between all experimental groups. Afterward, a post-hoc Tukey's test was achieved to compare means between pairs of treatment groups. *P ≤ 0.05 and **P ≤ 0.01 were reflected the significant.

RESULTS

X-ray diffraction analysis

In the present study the XRD pattern of the ternary bioactive glass (BAG) particles that prepared via three-step sol gel method, after heating at 700 °C for 2 h,⁽¹⁴⁾ The XRD pattern of the initial sample confirms its crystalline bioactive glass, (Fig. 1).

Particle size distribution

The laser diffraction method utilized for particle size analysis by the use or not use H₂O₂ pretreatment followed by 2 min ultrasound and 1-mm sieving was revealed for two soil samples and two aquatic sediments by examining ten replicates on a Malvern M2000 instrument. The carbon found was in the normal range for upland soils 0.1- 0.9% C, but one of the aquatic residue samples had a high carbon content (16.3% C) for which the H₂O₂ pretreatment was not practicable, (Fig. 2).

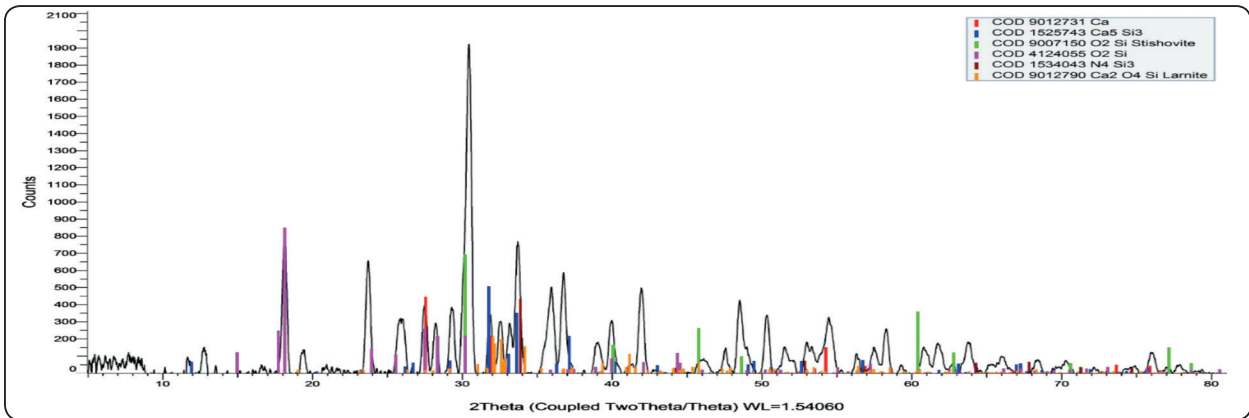


Fig. (1): XRD pattern of bioactive glass particles

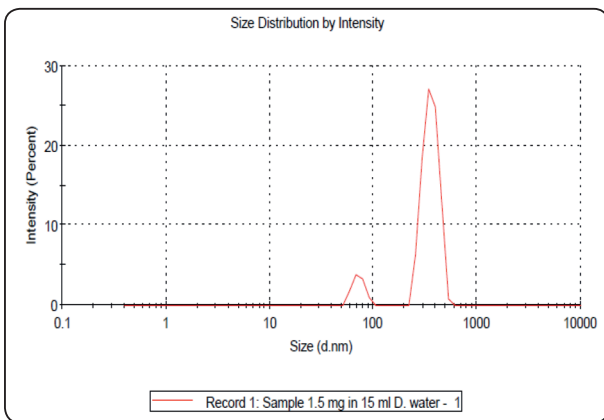


Fig. (2): Particle size distribution by volume of bioactive glass.

Histological results (H&E)

Microscopic examination of H&E-stained samples of **negative control** (normal) rats revealed compact bone tissue forms the shafts of femur bones, the bone tissue contained cellular lamellae with osteocytes, and the tissue was composed of vascular canals which radiated from the marrow cavity (Fig. 3 A). High magnification imaging of serial sections from the intervention site of **positive control** samples, performed **2 weeks** after the start of the experiment showed an intense inflammatory cell infiltrate, erythrocytes, new blood vessels and proliferating fibroblasts with formation of granulation tissue filled the bony defect of rats with appearance of fragments of defected bone but no

bone neoformation (Fig. 3 B).

While in the experimental groups, early processes of bone healing were observed. In **BAG group** rats where the bone defects were filled with bioactive glass (BAG), thin sparse immature bone trabeculae are present in the area of the bone defect in such a way to disrupt communication between the medullary channel and the outside. In **MTA group** rats where the bone defects were filled with MTA, bone trabeculae appeared to be thicker. The trabeculae were molded on the periosteum adjoining the bone defect. At the periphery of the defect, other trabeculae became separated from the internal part of the bone wall. The gaps between the trabeculae of bone were completely filled by the bone marrow rich in megakariocytes. In **TC group** rats where the bone defects were filled with TheraCal™ LC, the ossification process started from the edges of the cortical bone and progressed towards the center of the defect in the form of intercommunicating bone trabeculae with formation of exaggerated granulation tissue (Fig. 3 C, D, E).

However, examination under microscope of serial sections from the involved site, completed **5 weeks** at the beginning of the experiment displayed new bone formation along the borders of the surgical defect both in the positive control and experimental groups with regression of the inflammatory activity and less fibrous tissue in the region. Sparse

trabecular bone islands were observed in the bony defect of **positive control** rats (Fig.1 3 F). While, in **BAG group** rats, the formed bone seemed to be further remodeled, with a cortical exterior and internal marrow cavity. Moreover, in **MTA group** rats, at the surface of the experimental defect, the layer of proliferated bone is significantly thicker and reinforced. That it ensures restoration of bone continuity in the defective area. In **TC group** rats, typical bone formation seemed to be integrated or merged with the intact femur indicating complete bone healing and there is new a well-developed trabecular interior and cortical exterior. In this new bone, haversian structure was observed (Fig. 3 G, H, I).

Immunohistochemical detection of TNF- α

Examination of femur sections of negative control (normal) rats revealed negatively positive staining reaction of bone marrow tissue (Fig. 4 A). While, examination of specimens after **2 weeks** immunostained with TNF- α monoclonal antibody, exhibited strongly positive staining reactivity of bone marrow tissue of the positive control and three experimental groups with no significant difference (Fig. 4 B, C, D, E). In contrast, Negative to weak immunostaining reactivity of specimens after **5 weeks** was detected in the positive control and the three experimental groups with no significant difference (Fig. 4 F, G, H, I).

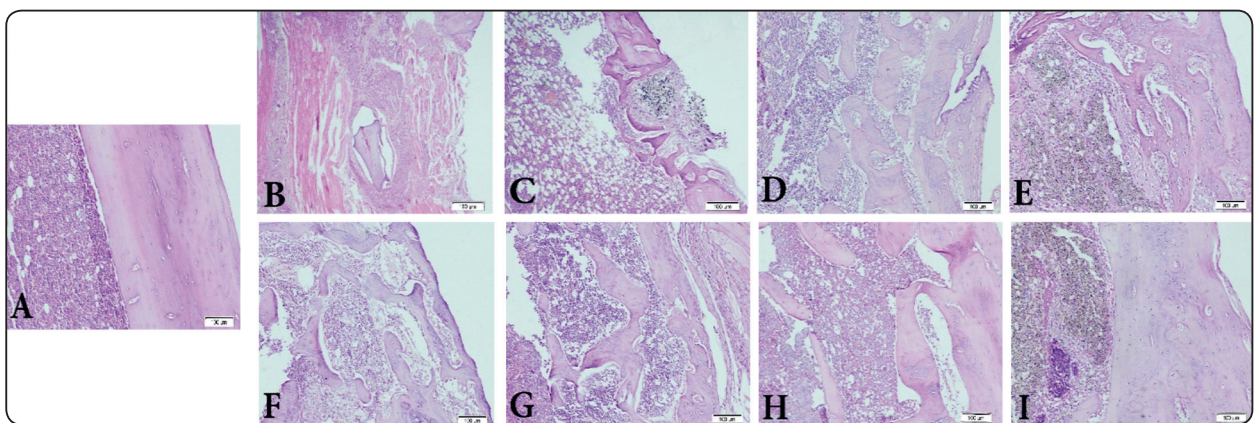


Fig. (3): Showing histological examination of femur bone of normal rats (A), positive control rats, BAG group rats, MTA group rats, TC group rats at 2 weeks (B, C, D, E) & at 5 weeks (F, G, H, I), (H&E).

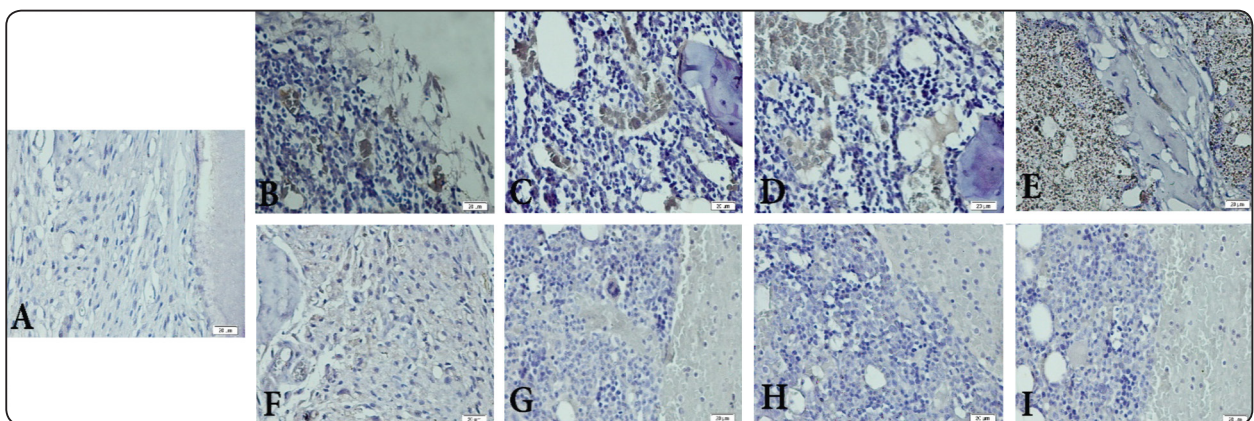


Fig. (4): Showing immunohistochemical localization of TNF- α of bone marrow tissue of femur bone of normal rats (A), positive control rats, BAG group rats, MTA group rats, TC group rats at 2 weeks (B, C, D, E) & at 5 weeks (F, G, H, I).

TABLE (1) Illustrates the mean labeling index of TNF- α in femur sections at the different groups:

	Positive control group	BAG group	MTA group	TC group
2 weeks	136.54 \pm 10.94	141.07 \pm 7.11	136.48 \pm 11.54	139.26 \pm 7.54
5 weeks	87.61 \pm 5.24	92.28 \pm 4.14	84.95 \pm 8.77	88.95 \pm 6.47
ANOVA-test	P \leq 0.05	P \leq 0.05	P \leq 0.05	P \leq 0.05

Data represented as mean \pm standard deviation.

Evaluation of TNF- α immunostaining by image analysis

There is high significant statistical difference (P \leq 0.05) between the positive control and three experimental groups at **2 weeks** when matched with those of the positive control and experimental groups at **5 weeks** using one-way ANOVA test. As the mean values are considered significant when the (P \leq 0.05). This means that the **TNF- α** immunostaining of bone marrow tissue of femur bone was gradually decreased at **5 weeks** for the experimental groups when compared with at **2 weeks** for the experimental groups, as shown in (Table 1).

DISCUSSION

In the present study, histological and immunohistochemical methods estimated the biocompatibility and osteoinductivity of different biomaterials including BAG, MTA & TC on bone healing of rat femurs.

The experimental groups showed early processes of bone healing with inflammatory cell infiltration in the area of the bone defect 2 weeks after the beginning of the experiment. While more osteoinductive effect with regression of the inflammatory activity and less fibrous tissue in the repaired region at the end of 5 weeks.

These results were in corroboration with a study ⁽¹⁶⁾ that reported the BAG is nontoxic to mouse osteoblast cells. Furthermore, BAG significantly initiated proteins as collagen type I, osteocalcin and osteopontin (induced genes) in 3 days of the cell culture.

Moreover, MTA induces hard tissue formation, remineralization, and production of transforming growth factor- β 1 due to its bioactivity ⁽¹⁷⁾.

Studies suggest that inflammation in the area of the bone defect with MTA is due to high alkalinity and is a reversible process ⁽¹⁸⁾. In a cell culture study observed adjustment of important odontogenic genes such as osteocalcin (OCN) and also improved secretion of vascular endothelial growth factor when MTA placed in hard tissue defects ⁽¹⁹⁾.

TC has displayed calcium release properties. Its ability to help in apatite formation may play a positive and critical role in hard tissue formation ⁽²⁰⁾.

TNF- α and linked molecules can promote cell survival or death according to the specific cell-surface receptor that join the cell type and the intracellular signaling cascade that is successively initiated⁽²¹⁾.

Immunohistochemical detection of TNF- α in our study revealed that **2 weeks** specimens exhibited clearly positive staining reaction of bone marrow tissue of the positive control and three experimental groups. In contrast, Negative to weak staining reaction of **5 weeks** specimens was observed in the positive control and three experimental groups.

These obtained results are in agreement with study ⁽²²⁾ presented, at 72 h time, TNF- α receptors, TNFR1 and TNFR2 are essentially conveyed by macrophages and other inflammatory cells. The TNF- α concentration peaks reached 24 h in mouse

models after bone injury, resuming to standard levels of healing of the involved fracture site

This brief TNF- α signals induced the delivery of secondary signaling molecules that initiate a chemotactic effect, employing the cells required for regeneration of bone⁽²³⁾. TNF- α concentration increased again around 3 weeks later, through endochondral bone formation. At that time, TNF- α is released by mesenchymal cells origin like osteoblasts, involving hypertrophic chondrocytes during endochondral bone formation. Deficiency of TNF- α , delayed endochondral bone formation and impairs fracture healing in mice for several weeks. Also, TNF- α deficient mice have normal skeletons, indicating that TNF- α signals is unique for postnatal fracture repair⁽²⁴⁾.

The histological and immunohistochemical evaluation of this study of bone healing in surgically created noncritical sized bone defects in rat femurs of the bioactive materials BAG, MTA & TC revealed bone formation with regression of the inflammatory activity and less fibrous tissue in the repaired region was seen 2 weeks and increased 5 weeks after their implantation.

In the biomaterial area for uses of bioactive materials that come in direct interaction with dental pulp stem cells (DPSCs) produces an environment that stimulates dentin like tissue formation by these enhanced cells. Furthermore, bioactive materials can serve for pulp capping that must be simply handled, workable, nontoxic, and capable of inducing dentin regeneration and repair⁽²³⁾. Moreover, the root-end filling material is an important element that may have an influence on the sequel of periapical surgery. Therefore, placement of a root-end filling is correlated with a significant better outcome^(25, 26).

Bioactive materials play an important role in treatment of situations like furcal perforation which is one of the utmost horrible and common accidents that can happen during endodontic treatment. Burs with inadequate direction and incompatible dimensions during access cavity preparation and

root canal location⁽²⁷⁾. Moreover, root resorption is an inflammatory response can be aggravated after pulp necrosis in the presence of bacteria or their by-products in the root canal system or in the dentinal tubules. The resorption process may lead to tooth loss⁽²⁸⁾.

The obtained results were in agreement with results of a study revealed that MTA and TC as pulp capping materials showed significant biocompatibility and low cytotoxicity⁽²⁹⁾. Also, BAG recorded a promising result through investigations on the pulp capping response on a rat model⁽³⁰⁾. One more study reported the relevance of BAG in endodontic treatment for pulp capping or partial pulpotomy⁽³¹⁾.

MTA mainly used in endodontic for pulp capping material, perforation repair, root-end fillings and creation of an apical barrier⁽³²⁾. **Lee et al**⁽³³⁾ compared pulp response to MTA and TC and recorded that TC produced less favorable pulpal responses than MTA response.

Recent research mentioned that TC allowed easily direct and indirect pulp capping procedure within a single appointment. Due to its controllable setting time, no problem of solubility and no need to mix or manipulate⁽³³⁾.

It should be emphasized that biocompatibility and osteoinductivity of the three bioactive materials (BAG, MTA & TC) recommended their applications in the field of endodontics.

CONCLUSION

BAG, MTA and TC bioactive materials are comparable to each other in their biocompatibility and showing absence of inflammation 5 weeks after their implantation in bony defects. Histological evaluation showed that MTA and TC materials are superior to BAG in terms of their bioactive properties. The biocompatibility besides osteoinductivity of BAG and TC supported their activity as pulp capping, root end filling materials and perforation repair like MTA.

ACKNOWLEDGEMENTS

The authors declare that they have no known competing financial interests or personal relationships that could have appeared to influence the work reported in this paper.

REFERENCES

1. Khalid MD, Khurshid Z, Zafar MS, Farooq I, Khan RS, Najmi A: Bioactive glasses and their applications in dentistry. *J Pak Dent Assoc.* 2017, 26: 32-38. <https://doi.org/10.25301/JPDA.261.32>.
2. Gerstenfeld LC, Cho TJ, Kon T, Aizawa T, Tsay A, Fitch J, Barnes GL, Graves DT, Einhorn TA: Impaired fracture healing in the absence of TNF- α signaling: the role of TNF- α in endochondral cartilage resorption. *J Bone Miner Res.* 2003, 18:1584-92. <https://doi.org/10.1359/jbmr.2003.18.9.1584>.
3. Lieberman JR, Daluiski A, Einhorn TA: The role of growth factors in the repair of bone biology and clinical applications. *J Bone Joint Surg.* 2002, 84: 1032-44. <https://doi.org/10.2106/00004623-200206000-00022>.
4. Pagni G, Kaigler D, Rasperini G, Avila-Ortiz G, Bartel R, Giannobile WV: Bone repair cells for craniofacial regeneration. *Adv Drug Deliv Rev.* 2012, 64: 1310-19. <https://dx.doi.org/10.1016%2Fj.addr.2012.03.005>.
5. Barnes GL, Kostenuik PJ, Gerstenfeld LC, Einhorn TA: Growth factor regulation of fracture repair, *J Bone Miner Res.* 1999,14: 1805-15. <https://doi.org/10.1359/jbmr.1999.14.11.1805>.
6. Fiume E, Barberi J, Verné E, Bains F: Bioactive Glasses from parent 45s5 composition to scaffold-assisted tissue-healing therapies. *J Funct Biomater.* 2018, 9: 24 <https://doi.org/10.3390/jfb9010024>.
7. Hench LL: The story of Bioglass. *J Mater Sci Mater Med.* 2006, 17:967-78. <https://doi.org/10.1007/s10856-006-0432-z>.
8. Salehi S, Gwinner F, Mitchell JC, Pfeifer C, Ferracane JL: Cytotoxicity of resin composites containing bioactive glass fillers. *Dent Mater.* 2015, 31: 195-203. <https://doi.org/10.1016/j.dental.2014.12.004>.
9. Funteas UR, Wallace JA, Fochtman EW: A comparative analysis of mineral trioxide aggregate and Portland cement. *Aust Endod J.* 2003, 29:43-4. <https://doi.org/10.1111/j.1747-4477.2003.tb00498.x>.
10. Asgary S, Eghbal MJ, Parirokh M: Sealing ability of a novel endodontic cement as a root-end filling material. *J Biomed Mater Res A.* 2008, 87:706-9. <https://doi.org/10.1002/jbm.a.31678>.
11. Masabni O, Wheeler M: Evaluation of calcium release from pulp-capping material using international organization for standardization guidelines. *J Adv Oral Res.* 2017, 8:57-62. <https://doi.org/10.1177%2F2229411217729085>.
12. Arandi NZ, Rabi T: TheraCal LC from biochemical and bioactive properties to clinical applications, *Int J Dent.* 2018 Mar 26; 2018:3484653. <https://doi.org/10.1155/2018/3484653>.
13. Camilleri J, Laurent P, About I: Hydration of Biodentine, TheraCal LC, and a prototype tricalcium silicate-based dentin replacement material after pulp capping in entire tooth cultures. *J Endod.* 2014, 40: 1846-54. <https://doi.org/10.1016/j.joen.2014.06.018>.
14. Hong Z, Reis RL, Mano L JF: Preparation and in vitro characterization of novel bioactive glass ceramic nanoparticles, *J Biomed Mater Res A.* 2009, 88: 304-13. <https://doi.org/10.1002/jbm.a.31848>.
15. Prasad BK, Chakravarthy M, Prabhu G: Applications of 'TissueQuant' a color intensity quantification tool for medical research. *Comput Methods Prog Biomed.* 2012, 106:27-36. <https://doi.org/10.1016/j.cmpb.2011.08.004>.
16. Yuan Z, Peng B, Jiang H, Bian Z, Yan P: Effect of bioaggregate on mineral-associated gene expression in osteoblast cells. *J Endod.* 2010, 36:1145-8. <https://doi.org/10.1016/j.joen.2010.03.025>.
17. Parirokh M, Torabinejad M: Mineral trioxide aggregate, a comprehensive literature review -Part III: Clinical applications, drawbacks, and mechanism of action. *J Endod.* 2009, 36:400-13. <https://doi.org/10.1016/j.joen.2009.09.009>.
18. Paranjpe A, Zhang H, Johnson JD: Effects of mineral trioxide aggregate on human dental pulp cells after pulp-capping procedures. *J Endod.* 2010, 36: 1042-7. <https://doi.org/10.1016/j.joen.2010.02.013>.
19. Bollu IP, Velagula D, Bolla N, Kumar K, Hari A, Thumu J: Histological evaluation of mineral trioxide aggregate and enamel matrix derivative combination in direct pulp capping: An *in vivo* study. *J Conserv Dent.* 2016, 19:536-40. <http://www.jcd.org.in/text.asp?2016/19/6/536/194031>
20. Gandolfi MG, Siboni F, Taddei P: Chemical-physical properties of TheraCal LC, a novel light-curable MTA-like

- material for pulp-capping. *Int Endod J*, 2012, 45: 571-9. <https://doi.org/10.1111/j.1365-2591.2012.02013.x>.
21. Locksley RM, Killeen N, Lenardo MJ: The TNF and TNF receptor super families: integrating mammalian biology. *Cell*. 2001, 104: 487-501. [https://doi.org/10.1016/s0092-8674\(01\)00237-9](https://doi.org/10.1016/s0092-8674(01)00237-9).
 22. Kon T, Cho TJ, Aizawa T, Yamazaki M, Nooh N, Graves D, Gerstenfeld LC, Einhorn TA: Expression of osteoprotegerin, receptor activator of NF-kappaB ligand (osteoprotegerin ligand) and related pro-inflammatory cytokines during fracture healing. *J Bone Miner Res*. 2001, 16:1004-14. <https://doi.org/10.1359/jbmr.2001.16.6.1004>.
 23. Gerstenfeld LC, Cullinane DM, Barnes GL, Graves DT, Einhorn TA: Fracture healing as a post-natal developmental process molecular, spatial, and temporal aspects of its regulation. *J Cell Biochem*. 2003, 88:873-84. <https://doi.org/10.1002/jcb.10435>.
 24. Tomas-Catala CJ, Collado-Gonzalez M, Garcia-Bernal D, Onate-Sanchez RE, Forner L, Llana C, Lozano A, Rodriguez-Lozano F.J. Biocompatibility of New Pulp-capping Materials NeoMTA Plus, MTA Repair HP, and Biodentine on Human Dental Pulp Stem Cells. *J Endod*. 2018, 44:126-32. <https://doi.org/10.1016/j.joen.2017.07.017>.
 25. Poggio C, Ceci M, Dagna A, Beltrami R, Colombo M, Chiesa M: In vitro cytotoxicity evaluation of different pulp capping materials: a comparative study. *Arh Hig Rada Toksikol*. 2015, 66: 181-8. <https://doi.org/10.1515/aiht-2015-66-2589>.
 26. Torabinejad M, Parirokh M, Dummer PM: Mineral trioxide aggregate and other bioactive endodontic cements: an updated overview-part II: other clinical applications and complications. *Int Endod J*. 2018, 51:284-317. <https://doi.org/10.1111/iej.12843>.
 27. Camilo do Carmo Monteiro J, Rodrigues Tonetto M, Coêlho Bandeca M, Henrique Borges A, Cláudio Martins Segalla J, Cristina Fagundes Jordão-Basso K, Fernando Sanchez-Puetate C, Carlos Kuga M: Repair of iatrogenic furcal perforation with mineral trioxide aggregate: a seven-year follow-up. *Iran Endod J*. 2017, 12:516-20. <https://doi.org/10.22037/iej.v12i4.16888>.
 28. Ashwini TS, Hosmani N, Patil CR, Yalgi VS: Role of mineral trioxide aggregate in management of external root resorption. *J Conserv Dent*. 2013, 16:579-81. <http://www.jcd.org.in/text.asp?2013/16/6/579/120937>.
 29. Christiansen R, Kirkevang LL, Horsted-Bindslev P, Wenzel A: Randomized clinical trial of root-end resection followed by root-end filling with mineral trioxide aggregate or smoothing of the orthograde gutta-percha root filling - 1-year follow-up, *Int Endod J*. 2009, 42:105-14. <https://doi.org/10.1111/j.1365-2591.2008.01474.x>.
 30. Long Y, Liu S, Zhu L, Liang Q, Chen X, Dong Y. Evaluation of pulp response to novel bioactive glass pulp capping materials. *J Endod*. 2017; 43:1647-50. <https://doi.org/10.1016/j.joen.2017.03.011>
 31. Skallefold HE, Rokaya D, Khurshid Z, Zafar MS: bioactive glass applications in dentistry. *Int. J. Mol. Sci*. 2019, 20: 5960. <https://doi.org/10.3390/ijms20235960>.
 32. Ha WN, Duckmanton P, Kahler B, Walsh LJ: A survey of various endodontic procedures related to mineral trioxide aggregate usage by members of the Australian Society of Endodontology. *Aust Endod J*. 2016, 42:123-38. <https://doi.org/10.1111/aej.12170>.
 33. Lee H, Shin Y, Kim SO, Lee HS, Choi HJ, Song JS: Comparative study of pulpal responses to pulpotomy with ProRoot MTA, RetroMTA, and TheraCal in Dogs' Teeth. *J Endod*. 2015, 41:1317-24. <https://doi.org/10.1016/j.joen.2015.04.007>
 34. Zarpade N, Gunda S, Patil A: TheraCal future of pulp capping. *IJDR*. 2017, 7:16338-42. <https://www.journalijdr.com/theracal%E2%80%A6-future-pulp-capping>.